

---

# SUPPLEMENTARY INFORMATION FOR

## Quantifying Tipping Risks in Power Grids and beyond

---

PREPRINT SUPPLEMENT

 **Martin Heßler\***

Institute for Theoretical Physics  
Westphalian Wilhelms-University Münster  
48149 Münster, North Rhine-Westphalia, Germany  
m\_hess23@uni-muenster.de

 **Oliver Kamps**

Center for Nonlinear Science  
Westphalian Wilhelms-University Münster  
48149 Münster, North Rhine-Westphalia, Germany  
okamp@uni-muenster.de

November 10, 2023

Corresponding author: Martin Heßler  
E-mail: m\_hess23@uni-muenster.de

**This pdf includes:**

- Supplementary text
- Infobox S1
- Figures S1 to S4

**Other supplementary materials for this manuscript include the following:**

- Data and simulation codes can be found at  
[https://github.com/MartinHessler/Disentangling\\_Tipping\\_Types](https://github.com/MartinHessler/Disentangling_Tipping_Types).
- The open-source package *antiCPy* is available at <https://github.com/MartinHessler/antiCPy> under a *GNU General Public License v3.0* and documented at <https://anticpy.readthedocs.io>.

---

\*Center for Nonlinear Science, Westphalian Wilhelms-University Münster, 48149 Münster, Germany

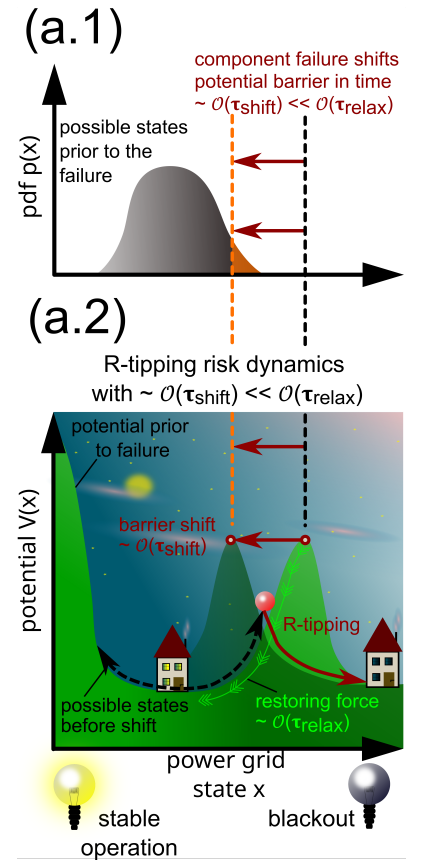
## Supplementary Information Text and Figures

### S1 Rate-dependent tipping

In our main article we focus on bifurcation-induced and noise-induced tipping events. For completeness we want to discuss the third of the commonly mentioned tipping routes, namely rate-dependent tipping (R-tipping), as well. In an R-tipping scenario a system undergoes a transition dependent on the rate of change of a control parameter. In such a case, a critical transition may occur without explicit consideration of bifurcations or noise levels at all. The rather subtle and fascinating phenomenon is sketched in Infobox S1, figure S1. During an R-tipping event the potential landscape can preserve its fixed points. Nevertheless, it modifies so fast on a time scale of order  $\mathcal{O}(\tau_{\text{shift}})$  that it exceeds the minimal required time for the system to follow the modifications driven by the potential's restoring force which lives on time scale  $\mathcal{O}(\tau_{\text{relax}})$ . Due to this discrepancy, the system's state is suddenly relocated in another basin of attraction if  $\mathcal{O}(\tau_{\text{shift}}) \ll \mathcal{O}(\tau_{\text{relax}})$  is sufficiently fulfilled. For power grids this could correspond to a rather sudden and substantial failure of multiple control units. Even if the failure of the control units over a broader time interval would have been manageable for the system's stability, falling out of all units in a very short time destabilizes the system by R-tipping. In principle, the Bayesian Langevin estimation (BL-estimation) procedure is related to the rate of change of a control parameter, since the slope of the drift slope estimates  $\hat{\zeta}$  resembles the control parameters changes of the drift term in a way. Nevertheless, the phenomenon of R-tipping is clearly out of reach for the method at that time for several reasons: Often R-tipping is barely resolved by definition, since the changes run off very fast. Based on this argument, the parameter changes have to be resolvable with the data information per window without producing a time delay due to the rolling window approach that is greater than the time scale of the R-tipping event itself. Furthermore the relations between the slopes of the drift slope estimates  $\hat{\zeta}$ , the control parameter change and the system-dependent critical ratio  $\frac{\tau_{\text{relax}}}{\tau_{\text{shift}}}$  are normally unknown.

#### Infobox S1: R-tipping scenario in power grids

Figure S1: Analogously to the Infoboxes 1 and 2, figures 1 and 2, the R-tipping mechanism is illustrated in the potential landscape. The gray probability density function (pdf) of the system state in subfigure (a.1) corresponds to the accessible positions of the red ball which lives in the light green potential at time  $t_0$  in subfigure (a.2). As indicated by the black arrow, the ball is confined in the stable operation valley of its potential prior to time  $t$ . The confinement is mastered by the restoring force (light green arrows) that corresponds to the steepness of the mountainside. If we consider the red ball without any external changes it would simply relax into the left valley with an intrinsic time scale of order  $\mathcal{O}(\tau_{\text{relax}})$ . However, in an ongoing R-tipping scenario the potential landscape is modified by a control parameter change on a much faster time scale  $\mathcal{O}(\tau_{\text{shift}})$  on which the gray pdf in (a.1) approximately remains stationary. In this sense, the specific ratio of  $\mathcal{O}(\tau_{\text{shift}}) \ll \mathcal{O}(\tau_{\text{relax}})$  is crucial for the R-tipping mechanism: Even if in principle the stable and unstable fixed points are preserved, they are shifted so fast that the red ball is unable to follow the shifted light green potential driven by its restoring force to relax to the left potential in a time comparable to  $\tau_{\text{shift}}$ . Instead, the potential landscape under the ball, which is almost stationary on the much faster time scale  $\tau_{\text{shift}}$ , changes into the shaded dark green potential. In consequence, the red ball feels the new restoring force that guides it to relax into the blackout state at time  $t_1$  slightly after the shifting time  $t$ . In a power grid this could happen for example due to a very abrupt and substantial failure of multiple control units so that the (possibly slightly perturbed) grid state cannot return into stable operation, although the remaining control units would normally be able to stabilize the grid, if they would have failed over an extended time interval instead of failing abruptly altogether.



## S2 Synthetic examples without time lag

In figure S2 the analysis results of the synthetic data is presented again, but the estimates are not related to the last time window point as in figure 4 of the main article. Instead the values are assigned to the mid points in time of each window to show that the estimates match the original model values marked by the green solid lines rather well in the Markov examples of figure S2 (a,d).

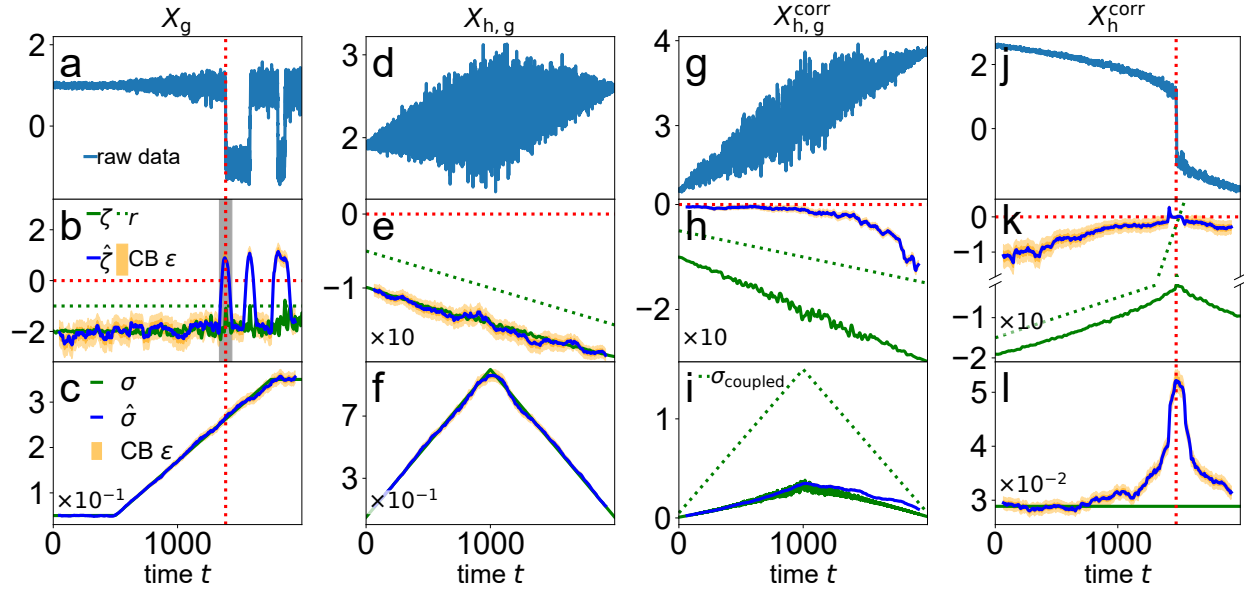


Figure S2: The figures show the BL-estimation results of the synthetic data examples of the main article, but instead of assigning the estimates of the method with the end point (cf. main article, figure 4), the estimates are assigned to the mid point of each window. This confirms the statement of rather accurate matching estimates with the real values in the Markov examples of figure S2 (a,d). Nevertheless, comparing the drift slope estimates in the correlated examples (h,k) to the analytical values (green solid lines) reveals that Non-Markovianity can lead to significantly biased estimates as expected keeping in mind the model assumptions.

## S3 Metadata Research

The two analysed time series of the North America Western Interconnection (NAWI) Blackout on 10th August 1996 which we analysed in section 2.2 of the main article were originally provided without corresponding metadata, i.e. absolute times and measurement locations. Available information only claimed both time series to be recorded with similar time resolution directly prior to the outage event [1–3]. We wondered about the significantly differing frequency measurements, since they were suggested to stem from the same period in time covering the same line of events. Since the power grid frequency is a macroscopic key observable of AC power systems which remains the same for all nodes, we expected to observe at least similar time evolution prior to the outage. There were mainly two hypotheses:

1. Both time series might have indeed covered the same time interval, but were measured at different locations. Following this idea, the differing frequency time evolutions might have been caused by topology features of the NAWI or might have been related to different islands that formed in course of the cascading event.
2. If the first hypothesis would not be true, the time series might have been erroneously claimed to cover the same period in time. Even if they both might correspond to the NAWI cascading failure on 10th August 1996, they would be related to different events in the outage cascade.

Furthermore, regardless of the actual outcome of the source's approval, it seemed to be an interesting project to dive into a detailed comparison between the analysis results and the real timeline of the historic blackout event. A check up of the data sources was necessary to dispel our doubts. The search spans roughly 1.5 a including intense correspondence with four institutions, i.e.

*Bonneville Power Administration* (BPA) via the *Freedom of Information Act* (FOIA) (correspondence with James King (FOIA Public Liaison, BPA) and Brian Roth (FOIA Case Coordinator, BPA)), *Western Electricity Coordinating Council* (WECC), the Washington State Library of the Office of the Secretary of State, Steve Hobbs, (correspondence with Mary Schaff (Librarian, Washington State Library) via the "Ask a Librarian Service") and the Seattle Municipal Archives.

In the beginning, we were provided with several data files from BPA which might have included the two time series and hopefully the missing metadata. Indeed, we could identify the pre-outage frequency record  $\omega_O(t)$  (cf. main article, figure 5) in one of the files. In further correspondence with BPA employees we could clarify that the record is measured in Tacoma and starts at 15:29:40 o'clock on 10th August 1996.

Unfortunately, the second time series shown in figure S3 (a) was not amongst the provided data files. Furthermore, we got the information that BPA measured frequency only in Tacoma and Dittmer at that time. Since Tacoma and Dittmer both belong to the Northern grid island and are separated by only  $\sim 220$  km, the new information largely excluded hypothesis 1. At this point, hypothesis 2 or some related error in the time scale became more likely. Since we knew that the second time series was digitized from a frequency time series scan from the *Western Systems Coordinating Council Disturbance Report* [4, 5] by other researchers [2, 3] in the field via a software tool, we reached out to them in order to receive the original scan, hoping to find notes about date and absolute times of the second dataset therein. We are grateful for the fast reply and the support of one of the authors. Unfortunately, he was not able to provide the original source, since the authors only got access to the printed responsive reports for a limited time period in 2012. However, he subsequently supported the search for the data source by valuable suggestions and discussions.

Thanks to a further BPA FOIA request we got the necessary reports. Though the version contains the list of Exhibits, it does not contain the actual figures and tables. Therefore, we reached out to WECC which was finally able to provide us with four pages of a frequency plot from the disturbance report. Unfortunately, the scan is of very low quality and the time axis is not readable. However, after carefully comparing the scan to our digitized version in figure S3 (a), we noticed that it matched up apart from some positive offset of the digitized frequency values on the right. We assumed that to be caused by the data extraction procedure from the low quality scan. Nevertheless, it nourished further doubt about the originally stated metadata: Based on these, the high peak of the frequencies in figure S3 (a) was declared to be the beginning of the outage event. The comparison to the low quality scan version showed that the frequencies in the black-hatched area are artificially lifted by the data extraction procedure and should line up at 60 Hz. Against that background, the originally stated metadata would have implied that the frequencies before the outage's peaks were less stable (flickered stronger around 60 Hz) than almost directly after the peak, when the blackout event already occurred. Furthermore, this stable frequency region would have been reached in the course of seconds to a few minutes, although after the historic NAWI outage on 10th August 1996 electric supply of all customers was restored over several hours until the next day and the grid was completely restored in the course of days until 16th August 1996. [4]

Subsequently, we identified the figure description of "Exhibit 10" in the disturbance report to correspond to the low quality scan. This enabled us to draft a more precise request to the Washington State Library via the "Ask a Librarian" service. Since Mary Schaff had only access to a scan of similarly disappointing quality in the Washington State Library, we asked her for alternative institutions which would hopefully archive a better resolved version. Finally, Mary Schaff reached out to several colleagues and got positive response from a colleague at the Seattle Municipal Archives. We are very grateful for the dedicated help of all the people who participated in solving the puzzle of the lost data source. Additionally, Mary Schaff let us have the timeline tables of the approved report's Exhibits, i.e. Exhibits two, three, five and nine, and her colleague from the Seattle Municipal archives sent us a full version of the preliminary report.

Unexpectedly, the readable time axis is labeled in daytime hours and disagrees significantly with the originally [2, 3] reported one. It spans almost a period of 20 h instead of 10 min of the *post*-outage period instead of the *pre*-outage period and time runs from right to left instead of vice versa. Since this strongly disagrees with the previously assumed setting, we tried to find notes in the preliminary and approved report about time scaling errors present in the frequency time series, but without success. Therefore, we summarize our arguments for the time scale which we assumed in the main article, section 2.2, in the following list.

#### Major Arguments:

1. We finally got the original source with readable time and frequency axes. They differ significantly from the originally assumed and reported [1, 3] setting. A search for notes about errors in the labelled axes in the approved and preliminary report was not successful. Furthermore, detailed information regarding the time scales, absolute times, and measurement locations for additional nine exhibits, which contain 63 more data plots, is consistently provided. The time axes runs from right to left which indicates that the frequency time series, used in previous articles [1–3, 6] and shown in figure S3 (a), should be inverted. Furthermore, the time series spans mostly the *post*-outage interval instead of the *pre*-outage period,

covers roughly 20 h instead of 10 min and is sampled 265 times less dense as expected from the originally reported dataset [2, 3].

2. The documented time scaling in the disturbance report fits exactly the time stamps of real events. For example, the first high peak is observed around the first islanding process at 15:49 o'clock. In particular, after 15:49 o'clock "the frequency stayed high in the Northern Island (about 60.4 Hz for 14 minutes, crossing 60 Hz after 17 minutes, dipping as low as 59.95 Hz, then rising to 60.04 Hz for the next 50 minutes)." [4] The easier available *North American Electric Reliability Corporation* (NERC) report describes the frequency time evolution as follows: "The North island frequency rose to 60.9 Hz dropping to 60.4 Hz within two seconds where it remained for about 14 minutes. The frequency crossed 60 Hz three minutes later." [7] Both descriptions fit perfectly the frequency time series assuming the scaling as stated in the approved disturbance report.
3. Based on the time scaling, documented in the approved report [4], we tried to align the presumed pre-outage segment (cf. black-hatched interval in figure S3 (a)) of the time series to frequency time series provided by BPA from which we knew absolute times and measurement location. The alignment suggests that the time series indeed resembles a record of roughly 20 hours mainly in the post-outage region. For more information about the alignment procedure we refer the reader to section S4.
4. The inverted time direction is further suggested by features of the time series if it is interpreted from right to left: Under this assumption the pre-outage frequencies are well-located around the expected stable 60 Hz and fluctuate stronger after the main blackout events indicating a less resilient and stable power grid state. Besides, the rather sudden separation of the islands is well-reflected by the sudden peak to roughly 60.4 Hz which relaxes towards 60 Hz again instead of increasing further in a saw tooth-shaped manner as the originally proposed time direction would suggest.
5. The originally assumed time stamps seem to be highly unlikely against the background that the corresponding time series shown in figure S3 (a) would indicate completely different frequency dynamics as the time series which were approved by BPA.

Apart from the above stated main arguments which focus on technical and empirical details of the time series in question, we thought about further arguments which we summarize as minor arguments.

#### **Minor Arguments:**

1. Probably the time series scan in the approved report [4] stems from a measuring device which printed the measured values directly to scale paper via a writing arm. Since, the scale papers axes are fixed, the printing direction, i.e. the time direction, is defined by the used scale paper and the calibration of the measuring device. This might explain why the time axis runs from right to left instead of the typical Western reading direction from left to right.
2. BPA did not find a data record corresponding to a request of pre-outage data. This might be due to the fact that the measurement was not stored in digital form, but only printed as stated above or due to the request which was based on the wrong assumption, namely searching for time series data like presented in figure S3 (a) *prior* to the outage in sub-second resolution, instead of mostly *after* the outage in second resolution.

Details of the time scale reconstruction are documented in the following section S4.

## **S4 Time Scale Reconstruction of the Post-Outage Frequency Time Series**

In the previous section S3 we summarize the intense research for the source of the post-outage frequency time series the analysis of which we present in the main article, section 2.2.2. After about 1.5 a, we finally got evidence for mistakes in the originally reported time scale in previous articles [1–3, 6]. The reasons for these errors are most likely twofold and closely related to the fact that it was digitized via a software package from a printed time series scan:

1. In most of the available sources, the time series scan is provided only in remarkably bad quality which impedes reading the time axis. Therefore, the time axis was presumably interpreted in the common Western reading sense, i.e. from left to right (cf. figure S3 (a)), instead of vice versa, which would have been correct for that scan. In addition, frequency peaks to 60.4 Hz occur in the erroneously defined "end" of the time series. This was most likely interpreted as the beginning of the outage for that reason and led to the fallacy that the time series scan covers mostly the pre-outage region.

2. As we know from correspondence with BPA the portable power system monitor (PPSM) which was used at that time recorded frequency in steps of 0.025 s. Probably, the researcher who extracted the digitized version from the scan had the same information about the PPSM's sampling step, because a step of 0.024 152 52 s was originally reported for the digitized version. [2, 3] In combination with the erroneously assumed Western reading sense of the time axis, this leads to the wrong interpretation of the time series to correspond to roughly 10 min of the pre-outage region.

However, for the reasons, stated in section S3, we assume that the time series in figure S3 (a) does not follow the red time axis orientation, but the green one. Furthermore, we know that the record covers almost 20 h instead of roughly 10 min, but cannot determine with certainty the absolute start time of the record by comparing the digitized version and the scale paper scan. For that reason, we need to reconstruct the sampling step as well as the absolute times of the record to allow for the comparison to the real timeline of events (cf. main article, section 2.2.2). To this end, we could have generated a time series from the scan based on the updated time scale information, e.g. with a software package like *DigitSeis* [8]. We did not follow this approach, but perform a comparison between the small pre-outage segment of the time series in question, i.e. the black-hatched segment in figure S3 (a) and two pre-outage time series which were provided by BPA with approved absolute times. To this end, we inverted the time series segment of interest, used an arbitrary time axis for this segment in the beginning and fixed one prominent point of coincidence between both the unknown time series from the scan and the known time series provided by BPA. In figure S3 (b) we show the time scale which we reconstructed based on the densely sampled time series of the original articles [2, 3]. Note that we used a thinned version with  $N_{\text{thin}} = 11300$  data points instead of the original one, containing  $N_{\text{dense}} = 23393$  samples to cancel artificial outliers in the subsequent analyses in the main article, section 2.2.2. The data was extracted during previous unpublished works of Kamps and Ehebrecht [1] from one of the low-quality scans without readable time axis. For more details about the outlier identification and treatment see section S7. Nevertheless, we performed the alignment to reconstruct the time scale with the densely sampled original version. For that reason, we have to convert the reconstructed time step  $\Delta t_{\text{dense}}$  into the thinned time step  $\Delta t_{\text{thin}}$  via

$$\Delta t_{\text{thin}} = \frac{N_{\text{dense}}}{N_{\text{thin}}} \cdot \Delta t_{\text{dense}} = 2.07 \cdot \Delta t_{\text{dense}} \quad (\text{S.1})$$

in order to get the correct time step of the BL-estimation analysis, presented in the main article, section 2.2.2. We fixed the points exactly before the reported 59.9 Hz to 59.95 Hz frequency dip as indicated by the red star. Because the extracted data display a 60 Hz offset prior to the frequency dip, which is not present in the original time series scan, we calculate the average data offset from 60 Hz for all data points before the first black dot and subtract it from the raw digitized version. A similar, artificial offset is found in the peak region referred to 60.4 Hz. Therefore, we average the offsets for all points beginning with the grey dot and subtract the result from the data segments starting with the second black dot. The small shift between the grey and second black dot is necessary, because the digitized data deviate slightly from the printed ones in the peaking region. However, the assumed shift is only an approximation.

In a final step, we stretched and compressed the arbitrary time scale of the blue time series in question by keeping it fixed at the red star position. In that way, we could try various alignments between the approved time series and the blue time series which was digitized from the report scan. The subjectively defined best fit is given by the alignment in figure S3 (b) which is subsequently used for further treatment prior to the analyses in section 2.2.2 of the main article. The alignment corresponds to the time series in question,

- starting at 15:10:45 o'clock on 10th August 1996
- with a time step of  $\Delta t_{\text{dense}} = 3.096\,137$  s, i.e.  $\Delta t_{\text{thin}} = 6.41$  s.

We also show two alternative alignments in figure S3 (c, d) to demonstrate the uncertainties in this approach. However, the variation of the time step are of maximum order  $\mathcal{O}(10^{-1}\text{s})$  and the start times 15:11:00 and 15:09:30 o'clock in the figures S3 (c) and (d), respectively, combined with the results from section S6, suggest that the start time's uncertainty is roughly  $\sigma_{t_s} = \pm 3$  min. Thus, the variations should not influence our results in the order of hours. Apart from yielding a suitable time axis for the actual analysis of the data, the approach can be seen as an additional argument for the time scale and time direction assumed in our article which clearly differs from previous studies [1, 2, 6, 9].

## S5 Frequency dip and changing grid state

The time stamp of the first pre-outage change of the power grid state, as indicated by the BL-estimation in figure 5 (b,c), is marked as a dark red dashed vertical line in figure S3 (b-d). The time stamp falls together with the downwards trend of a frequency dip, best visible in the green and orange pre-outage time series from BPA. The frequency dip might indicate sudden load increase that might be triggered by the beginning of the Keeler-Allston line's tree-related high impedance fault or by another reason. Even if the

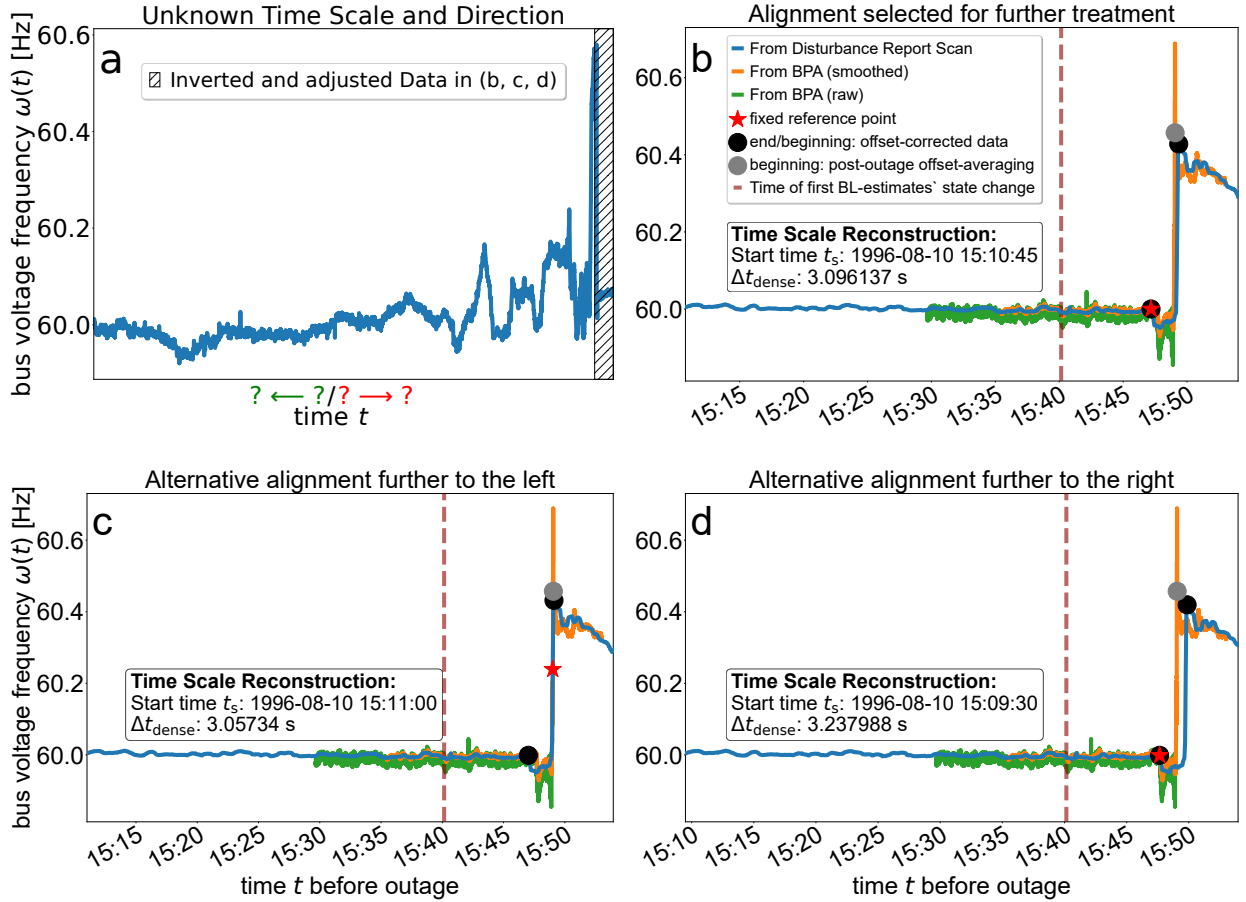


Figure S3: Reconstruction of the unknown time axis of the post-outage time series analysed in the main article's section 2.2.2, figure 5 (d-f). (a) Originally, the blue time series was reported to cover roughly 10 min of the pre-outage time interval of the NAWI cascading failure on 10th August 1996 from left to right with time step  $\Delta t = 0.024\ 152\ 52\text{s}$ . An extensive search for the data source (cf. section S3) doubted the integrity of the originally assumed axis and suggested an inverted time direction, i.e. the green instead of the red-marked x-axis direction. Furthermore, the recovered data source suggests that only the small black-hatched interval corresponds to the pre-outage period. (b) Therefore, we used the inverted data from the black-hatched region to align it to approved pre-outage time series with known time scale and absolute times from BPA (green and orange). Initially, both the known and unknown time series are aligned to a prominent point, marked by the red star, using an arbitrary time axis for the blue time series in question. After fixing the alignment of the time series, the time step of the blue time series is adjusted to best match the approved pre-outage data from BPA. The starting time of the record and the sampling step extracted in this way are printed in the text box. Note that the data prior to the 59.9 Hz to 59.95 Hz dip as well as the data of the 60.4 Hz peak exhibit artificial offsets compared to the original source and are most likely due to the process of digitization of the time series from a scan. Against that background, we corrected the affected pre-outage interval from beginning of the time series to the first black point by an offset average referred to 60 Hz. Similarly, we took the average of the peak interval data compared to 60.4 Hz starting with the grey dot. The data behind the second black dot are offset-corrected by the peak interval offset-average. The shift between the grey and black dot is to approximately account for time scaling discrepancies in the peaking region due to the data extraction. (c,d) Alternative alignments achieved analogously to (b). The alternative alignments demonstrate that the procedure leads to uncertainties of the time step of  $\mathcal{O}(10^{-1}\text{s})$  and suggests a deviation of the starting time within less than one minute. Combined with the results of section S6, the maximum uncertainty of the starting time is  $\sigma_{t_s} = 3\text{ min}$ . That suggests that the actually chosen alignment has no influence on the results stated in section 2.2.2 of the main article.

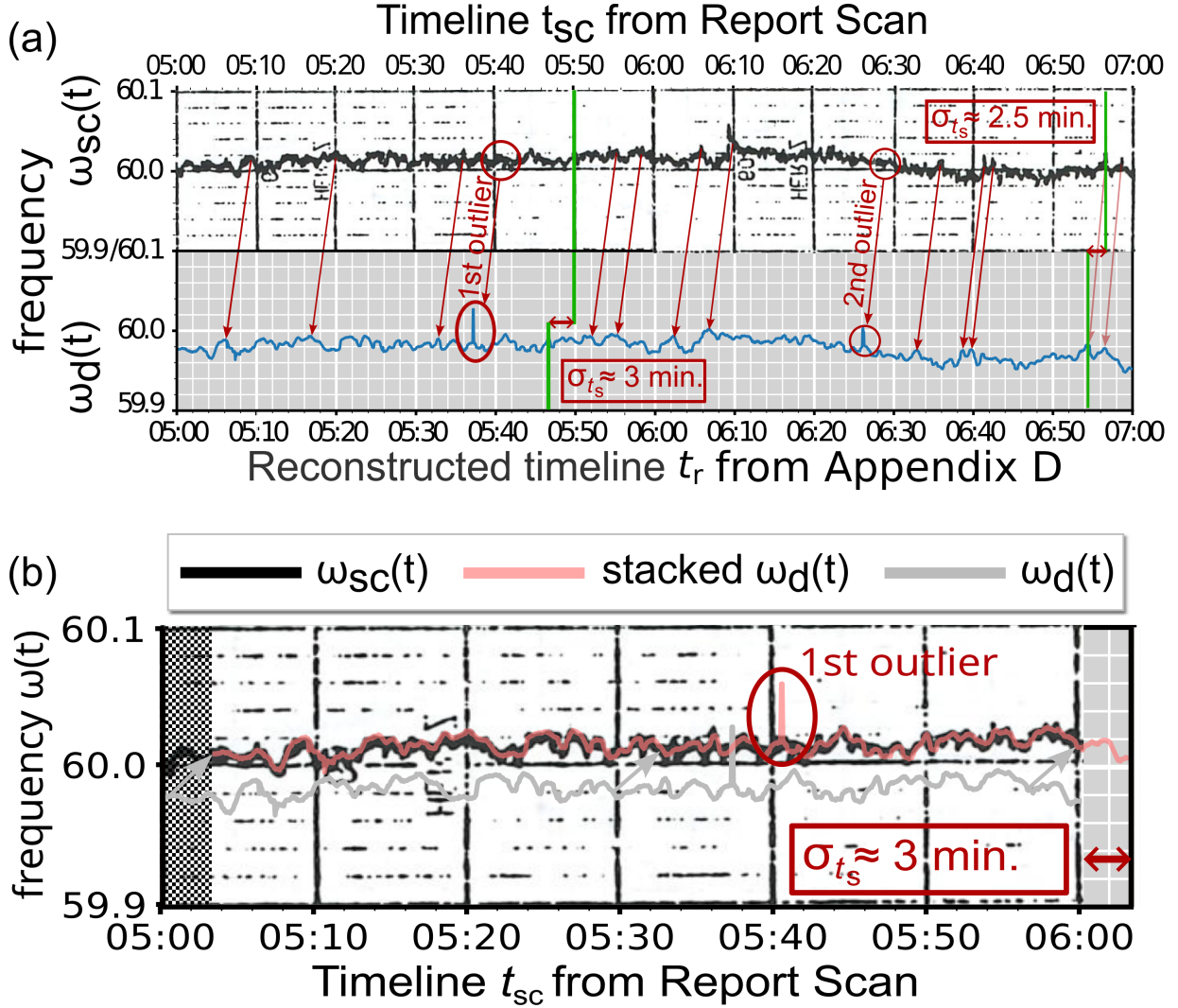


Figure S4: Identification of outlier regions and estimation of the uncertainty that adheres the start time estimate of the post-outage frequency time series (cf. section S4). The densely sampled time series is used for comparison, but all conclusions stated here hold also for the thinned version. The scale ratio of the digitized time series in the lower graph is adjusted to the one of the upper screenshot of the analog time series for easy comparison. (a) Comparison between the printed original frequency time series  $\omega_{sc}(t)$  and its digitized twin  $\omega_d(t)$ . The outlier regions are signed by red circles and ellipses. The prominent peaks in the digitized version are artefacts due to misinterpreting the scale paper major grid lines as data points during data extraction by an adequate software. The two highlighted peaks are treated by the procedure described in the main article, section 7. Smaller ones without significant impact remain, as e.g. the two sharp dips directly behind the first red arrow beginning from the left. Prominent points for the comparison of both time series are highlighted by the red arrows. They mark a discrepancy between the reconstructed time scale and the time step, derived by the procedure described in section S4. We measured the resulting uncertainty  $\sigma_{ts}$  of the reconstructed start time  $t_s$  by determining the time interval between two of the prominent points in both time series, marked by the green lines. The maximum uncertainty is  $\sigma_{ts} = 3 \text{ min.}$  Note that the absolute frequency values of the digitized version exhibit a negative offset of roughly  $0.02 \text{ Hz}$  in the considered interval. (b) We additionally compare the first outlier region by stacking both time series segments one above the other. Note that the frequency scaling of the digitized version  $\omega_d(t)$  is lost that way. Anyways, it is an additional way to measure the uncertainty of the start time estimate  $t_s$ . The digitized red version is shifted to the right to agree with the time scale of the report as visible by the black-tiled area in the beginning without digitized data and the overhang in the end. The overhang is used to determine the uncertainty again, which fits the results of the previous approaches. The minute scale uncertainty is irrelevant for the conclusions in the main article which live on a scale of hours.

actual reason cannot be deduced with certainty, the comparison suggests a relation between the frequency dip and the permanent grid state change found with the BL-estimation method roughly 2 min prior to the officially declared triggering event of the historic NAWI cascading failure on 10th August 1996.

## S6 Start time uncertainty estimate of the post-outage frequency time series

The comparison of the outlier regions in figure S4 reveals that the reconstructed time scale, derived in section S4, includes the uncertainty  $\sigma_{t_s} = 3$  min. It is determined by adjusting the scale ratio of the digitized frequency time series  $\omega_d(t)$  to the screenshots of the original, analog time series  $\omega_{sc}(t)$  of the scan for easy comparison. The misalignment is highlighted by comparing prominent time series patterns, indicated by the red arrows. The discrepancy of two of such patterns is measured between the green lines, resulting in a misalignment of maximum  $\sigma_{t_s} = 3$  min. Another approach to control this is shown in figure S4 (b). Both time series are stacked one above the other, with the digitized version shifted to the right to match up with the time scale of the report scan. This shift is measured by the protruding end of the time series and yields the same results. Since the analysis in the main article, section 2.2.2, lives on a scale of hours, this uncertainty does not affect the conclusions in any way.

## S7 Identification of artificial outliers in the post-outage frequency

We noticed strange artefacts in the BL-estimation results, namely discontinuous jumps of the slope  $\hat{\zeta}$  and noise estimates  $\hat{\sigma}$  to values that remained constant over rather exactly one window length, before they returned almost to the previous value. Based on this observation, we inspected the affected time series periods carefully by eye. Therefore, we zoomed into the affected periods of time and found actually strong outlier shocks. After receiving the approved report's frequency time series scan [4]  $\omega_{sc}(t)$  from Exhibit 10, we were able to compare the original printed version  $\omega_{sc}(t)$  to the digitized version  $\omega_d(t)$ . In figure S4 we provide a comparison of the time segment of interest, i.e. from 05:00 to 07:00 o'clock on 11th August 1996. For easy comparison we adjusted the scale ratio of the digitized frequency time series  $\omega_d(t)$  to the one given by the snapshots of the printed frequency scan  $\omega_{sc}(t)$ . Note that there is a time series shift in figure S4 (a) due to the approximate reconstruction of the start time of the post-outage frequency data in section S4. More details on the start time uncertainty and the observed shift about 3 min can be found in section S6. Accounting for that shift, we identified the corresponding regions in both, the original printed frequency data  $\omega_{sc}(t)$  and the digitized one  $\omega_d(t)$ , marked by the red circles and ellipses in figure S4 (a). The first outlier is additionally signed in figure S4 (b) which provides the most comfortable way of comparison by laying both equally scaled time series directly one above the other. However, we preferred to show presumably figure S4 (a) to emphasize that the *total* values of the frequencies are only approximately reconstructed. Basically, the digitized frequencies  $\omega_d(t)$  are negatively shifted by an offset of roughly 0.02 Hz. Summarized, the outliers are generated by the digitizing software that tends to misinterpret the scale paper grid, especially the major lines as data points. The denser the chosen sampling, the stronger the effect. For that reason, we use a digitized version with only 11300 data points instead of the original version with 23393 data points that is used in previous articles [1–3, 6]. In doing so, we cancel already 4 of six prominent outliers from the data generation procedure, even though smaller ones with less impact remain, as e.g. the two sharp dips in the downwards trend of the frequency directly behind the first red arrow from the left. They are most likely caused by the minor grid lines. The remaining two outliers which we highlighted in figure S4 are treated by the procedure described in the main article, section 7. Briefly, the outliers are replaced by random values of a suitable range.

## SI References

- [1] Ehebrecht, F. *Anticipation of critical transitions in complex systems*. Master's thesis, Westphälische Wilhelms-Universität Münster (2017).
- [2] Hines, P., Cotilla-Sánchez, E. & Blumsack, S. Topological models and critical slowing down: Two approaches to power system blackout risk analysis. In *2011 44th Hawaii International Conference on System Sciences*, DOI: 10.1109/hicss.2011.444 (IEEE, 2011).
- [3] Cotilla-Sánchez, E., Hines, P. D. H. & Danforth, C. M. Predicting critical transitions from time series synchrophasor data. *IEEE Transactions on Smart Grid* **3**, 1832–1840, DOI: 10.1109/tsg.2012.2213848 (2012).
- [4] Watkins (BPA), D. *et al.* Western Systems Coordinating Council. Disturbance Report. For the Power System Outage that Occurred on the Western Interconnection. August 10, 1996. 15:48 PAST. Approved by the WSCC Operation Committee on October 18, 1996 (1996). The text source without Appendices was provided by Bonneville Power Administration via a Freedom of Information Act request thanks to James King (FOIA Public Liaison, BPA) and Brian Roth (FOIA Case Coordinator, BPA).

The Appendices 2,3,5,9 of the timeline were provided thanks to Mary Schaff from the Washington State Library, operating under the Secretary of State, Steve Hobbs, via mail correspondence with the "Ask a Librarian". (Washington State Library, Point Plaza East, 6880 Capitol Blvd. SE, Tumwater, PO Box 42460, Olympia WA 98504-2460, Phone: (360) 704-5200, Email: askalibrarian@sos.wa.gov). A low quality scan of the restoration frequency time series from the approved report's Exhibit 10 was provided by WECC, a readable version from the preliminary report by the Seattle Municipal Archives (Seattle Municipal Archives, 600 Fourth Avenue, Third Floor, Seattle, WA, 98104, PO Box 94728, Seattle, WA, 98124-4728, Phone: (206) 684-8353, Email: archives@seattle.gov). The contact to the Seattle Municipal Archives was established by Mary Schaff.

- [5] WSCC Investigative Task Force. WSCC Preliminary System Disturbance Report. August 10, 1996. 15:48 PAST (1996). The source was provided via mail correspondence thanks to the Seattle Municipal Archives (Seattle Municipal Archives, 600 Fourth Avenue, Third Floor, Seattle, WA, 98104, PO Box 94728, Seattle, WA, 98124-4728, Phone: (206) 684-8353, Email: archives@seattle.gov). Contact was made thanks to Mary Schaff from the Washington State Library, operating under the Secretary of State, Steve Hobbs. (Washington State Library, Point Plaza East, 6880 Capitol Blvd. SE, Tumwater, PO Box 42460, Olympia WA 98504-2460, Phone: (360) 704-5200, Email: askalibrarian@sos.wa.gov).
- [6] Grziwotz, F. *et al.* Anticipating the occurrence and type of critical transitions. *Sci. Adv.* **9**, DOI: 10.1126/sciadv.abq4558 (2023).
- [7] Eakeley, E. C. *et al.* 1996 System Disturbances. Review of Selected 1996 Electric System Disturbances in North America. <https://www.nerc.com/pa/rrm/ea/SystemDisturbanceReportsDL/1996SystemDisturbance.pdf> (Retrieved: 13 April 2023) (2002). North American Electric Reliability Council. Princeton Forrestal Village 116-390 Village Boulevard Princeton, New Jersey 08540-5731.
- [8] Ishii, M. & Ishii, H. DigitSeis: software to extract time series from analogue seismograms. *Prog. Earth Planet. Sci.* **9**, DOI: 10.1186/s40645-022-00508-0 (2022).
- [9] Corrado, R., Cherubini, A. M. & Pennetta, C. Early warning signals of desertification transitions in semiarid ecosystems. *Phys. Rev. E* **90**, DOI: 10.1103/physreve.90.062705 (2014).